

A Model of Overall Survival Predicts Treatment Outcomes with Atezolizumab versus Chemotherapy in Non-Small Cell Lung Cancer Based on Early Tumor Kinetics



Laurent Claret¹, Jin Y. Jin², Charles Ferté³, Helen Winter², Sandhya Girish², Mark Stroh², Pei He⁴, Marcus Ballinger⁵, Alan Sandler⁵, Amita Joshi², Achim Rittmeyer⁶, David Gandara⁷, Jean-Charles Soria³, and René Bruno¹

Abstract

Purpose: Standard endpoints often poorly predict overall survival (OS) with immunotherapies. We investigated the predictive performance of model-based tumor growth inhibition (TGI) metrics using data from atezolizumab clinical trials in patients with non-small cell lung cancer.

Patients and Methods: OS benefit with atezolizumab versus docetaxel was observed in both POPLAR (phase II) and OAK (phase III), although progression-free survival was similar between arms. A multivariate model linking baseline patient characteristics and on-treatment tumor growth rate constant (KG), estimated using time profiles of sum of longest diameters (RECIST 1.1) to OS, was developed using POPLAR data. The model was evaluated to predict OAK outcome based on estimated KG at TGI data cutoffs ranging from 10 to 122 weeks.

Results: In POPLAR, TGI profiles in both arms crossed at 25 weeks, with more shrinkage with docetaxel and slower KG with atezolizumab. A log-normal OS model, with albumin and number of metastatic sites as independent prognostic factors and estimated KG, predicted OS HR in subpopulations of patients with varying baseline PD-L1 expression in both POPLAR and OAK: model-predicted OAK HR (95% prediction interval), 0.73 (0.63–0.85), versus 0.73 observed. The POPLAR OS model predicted greater than 97% chance of success of OAK (significant OS HR, $P < 0.05$) from the 40-week data cutoff onward with 50% of the total number of tumor assessments when a successful study was predicted from 70 weeks onward based on observed OS.

Conclusions: KG has potential as a model-based early endpoint to inform decisions in cancer immunotherapy studies. *Clin Cancer Res*; 24(14): 3292–8. ©2018 AACR.

Introduction

Atezolizumab is an engineered humanized immunoglobulin G1 monoclonal antibody that targets programmed death-ligand 1 (PD-L1) to block the interaction with its receptors programmed death-1 (PD-1) and B7.1, thereby restoring tumor-specific T-cell immunity (1–4). Targeting PD-L1 with atezolizumab may preserve immune homeostasis in normal tissue by leaving the

programmed death-ligand 2 (PD-L2)/PD-1 interaction intact (5, 6). PD-L1 is expressed on tumor cells (TC) and tumor-infiltrating immune cells (IC) on a wide variety of cancers, and atezolizumab has demonstrated clinical efficacy against many different tumor types (4).

Atezolizumab is approved in the United States for the treatment of metastatic urothelial carcinoma and metastatic non-small cell lung cancer (NSCLC). The open-label randomized controlled trials POPLAR (7) and OAK (8), comparing atezolizumab versus docetaxel, have been conducted in patients with advanced pretreated NSCLC. Both studies showed an overall survival (OS) benefit of atezolizumab compared with docetaxel, whereas the objective response rate (ORR) and progression-free survival (PFS) were similar between treatment groups. Increasing improvement in OS was associated with increasing PD-L1 expression (on TCs and tumor-infiltrating ICs) in POPLAR with no benefit in patients with low or no expression (7). In OAK, OS was improved [median OS of 13.8 months (95% confidence interval, CI, 11.8–15.7) for atezolizumab versus 9.6 months (8.6–11.2) for docetaxel HR of 0.73 (95% CI, 0.62–0.87), $P = 0.0003$] regardless of PD-L1 expression levels, whereas patients with high expression derived the greatest OS benefit (HR) (8). In addition, a nonrandomized phase II study, BIRCH (9), demonstrated responses with atezolizumab monotherapy in patients with PD-L1-selected advanced NSCLC across lines of therapy.

¹Clinical Pharmacology, Roche/Genentech, Marseille, France. ²Clinical Pharmacology, Roche/Genentech, South San Francisco, California. ³Gustave Roussy, Villejuif, France. ⁴Biostatistics, Roche/Genentech, South San Francisco, California. ⁵Clinical, Roche/Genentech, South San Francisco, California. ⁶Lungenfachklinik Immenhausen, Immenhausen, Germany. ⁷University of California, Davis, Davis, California.

Note: Supplementary data for this article are available at Clinical Cancer Research Online (<http://clincancerres.aacrjournals.org/>).

Current address for C. Ferté and J.-C. Soria: AstraZeneca-MedImmune, Gaithersburg, Maryland.

Current address for M. Stroh: CytomX Therapeutics, South San Francisco, California.

Corresponding Author: René Bruno, Roche/Genentech, 84 Chemin des Grives, 13013 Marseille, France. Phone: 33-677-89-5298; Fax: 33-491-42-7397; E-mail: rene.bruno@roche.com

doi: 10.1158/1078-0432.CCR-17-3662

©2018 American Association for Cancer Research.

Translational Relevance

There is a need for novel endpoints to support decisions in clinical trials with immunotherapies. Model-based estimates of on-treatment growth rate constant (KG, using longitudinal tumor size data per RECIST 1.1) predict overall survival (OS) benefit (HR) with atezolizumab versus docetaxel in non-small cell lung cancer. A multivariate OS model with albumin and number of metastatic sites as independent baseline prognostic factors and estimated KG based on phase II POPLAR study is proposed and externally validated in predicting phase III study OAK OS HR (in all comers as well as by PD-L1 expression) based on early tumor kinetic data (40 weeks) before OS maturation. In both studies, progression-free survival was similar between arms. Model-based estimates of on-treatment growth rate constant may provide an early endpoint to support decisions in cancer immunotherapy studies.

Longitudinal tumor size models have been proposed to estimate tumor growth inhibition (TGI) metrics based on the sum of longest diameters (SLD) of target lesions per RECIST (10). TGI metrics predict for OS as shown in colorectal cancer (11, 12), NSCLC (13, 14), and several other tumor types for a variety of treatments (15). These models, at a minimum, capture the competing rates of tumor size growth and shrinkage with or without delay in treatment effect. In the case of cancer immunotherapy (CIT), the dynamics of tumor response to treatment may not necessarily be the same as seen with other mechanisms of action. Response patterns with CIT are potentially diverse; delayed responses and an initial increase in tumor burden or appearance of new lesions before regression (pseudoprogession) have been observed (16). Preliminary findings indicate that more patients with metastatic melanoma may show pseudoprogession, when defined as radiographic response following initial progression ($\approx 10\%$) (16–18), compared with other tumor types such as NSCLC, for which isolated occurrences are reported with an approximate overall incidence of 4% in 1,126 patients (17).

Although cases of dramatic pseudoprogession appear to be rare, the observation that OS is improved in NSCLC with anti-PD-L1/PD-1 therapies relative to chemotherapy, despite similarities in PFS and ORR (7, 8), implies that RECIST-based endpoints may not adequately measure efficacy in a way that predicts survival benefit for this class of treatment because of CIT duration of response, prolonged decreased growth kinetics, or other nonclassical response patterns. A model-based tumor kinetic approach may provide a complementary assessment of response in addition to the Immune-Related Response Criteria (16, 18, 19) to account for unconventional responses to CIT.

The aim of the investigation was to model the relationships between TGI metrics and OS based on phase II study POPLAR data, to perform external validations of the model (phase II BIRCH, phase III OAK), and finally to evaluate the model to predict OAK outcome based on early tumor kinetic data cutoffs.

Patients and Methods

Data

Analyses were conducted using data from the two randomized, open-label studies of atezolizumab versus docetaxel

in patients with NSCLC who progressed during or following prior platinum chemotherapy (POPLAR and OAK studies). Patients in POPLAR and OAK were randomly assigned (1:1) to receive i.v. atezolizumab (1,200 mg) or docetaxel (75 mg/m²) once every 3 weeks. In the BIRCH study, all patients received i.v. atezolizumab (1,200 mg) every 3 weeks without any comparison treatment group. Patients were either first-line (no prior chemotherapy for advanced disease; cohort 1), second-line (progression during or following ≤ 1 prior platinum-based regimen for advanced disease; cohort 2), or third-line or more (progression during or following ≥ 2 prior chemotherapy regimens for advanced disease; cohort 3). Full details on the protocols, consort diagrams, and results were described previously (7–9). These studies were conducted in accordance with the Declaration of Helsinki after approval by institutional review boards or independent ethics committees. All patients provided written informed consent.

Baseline PD-L1 expression was scored by immunohistochemistry according to previously published scoring criteria (7) as percentage of PD-L1-expressing TC (TC3 $\geq 50\%$, TC2 $\geq 5\%$ and $< 50\%$, TC1 $\geq 1\%$ and $< 5\%$, and TC0 $< 1\%$) and as percentage of PD-L1-expressing tumor area for IC (IC3 $\geq 10\%$, IC2 $\geq 5\%$ and $< 10\%$, IC1 $\geq 1\%$ and $< 5\%$, and IC0 $< 1\%$).

TGI model

A previously published biexponential TGI model (20) was used to fit tumor size data (SLD per RECIST 1.1) (10) and estimate on-treatment shrinkage rate (KS) and growth rate constants (KG). The model was implemented as follows (12). To capture delayed response, a time lag (delay) on onset of effect was tested in the model.

$$TS(t) = \begin{cases} TS_0 \cdot [\exp(KG \cdot (t - \text{tlag})) - 1] & \text{if } t < \text{tlag} \\ TS_0 \cdot [\exp(-KS \cdot (t - \text{tlag})) + \exp(KG \cdot (t - \text{tlag})) - 1] & \text{if } t \geq \text{tlag} \end{cases}$$

Where t is the time (week); TS is the tumor size (SLD in mm), tlag is the lag time for treatment onset; TS_0 at start of treatment + tlag: $TS(0 + \text{tlag})$; KG is the tumor growth rate constant (week⁻¹); KS is the tumor shrinkage rate constant (week⁻¹). A lognormal distribution was assumed for interindividual variability on each of the parameters as well as a normally distributed additive error for residual variability with mean 0 and variance σ^2 . A mixture model was also tested for tlag with two subpopulations, one with tlag fixed at 0 and one where tlag is estimated. Parameters of the model were estimated with a nonlinear mixed effect (population) approach (NONMEM, version 7.3.0) using the first-order conditional estimation algorithm with interaction (21). Asymptotic standard errors of parameter estimates were reported. Individual parameters were estimated after estimating the population parameters using *post hoc* Bayesian estimation in NONMEM (21). Stability of the model parameter estimates was evaluated using a bootstrap approach (Wings for NONMEM, <http://wfn.sourceforge.net/index.html>).

The following individual TGI metrics were estimated and tested as predictors of OS:

- TGI model parameter estimates: KG, KS
- Early change in tumor size (ECTS_x) as: $ECTS = TS(\text{week}_x)/TS(0)$ where $x = 6, 12, 14, \text{ or } 16$
- Time to growth (TTG) as: $TTG = (\text{LogKS} - \text{LogKG}) / (\text{KS} + \text{KG}) + \text{tlag}$

The TGI model was developed based on the POPLAR data and applied to the OAK or BIRCH data to estimate TGI parameters and metrics.

Statistical analyses

The OS model was developed based on POPLAR data. OS data were explored using the Kaplan–Meier estimation and Cox regression analyses (using *survfit* and *coxph* functions, respectively, in R, version 3.1.3). The following baseline patient characteristics were tested to explain variability in OS [age, sex, body weight, Eastern Cooperative Oncology performance status, smoking status (never smokers vs. other), total protein, albumin, alkaline phosphatase, aspartate aminotransferase, lactate dehydrogenase, tumor size (SLD), number of metastatic sites, histology (nonsquamous vs. squamous), years since metastasis, and PD-L1 expression] as well as treatment-related variables (treatment arm and TGI metrics).

A parametric survival regression model (using the *survreg* function in R, version 3.1.3) was developed to describe the baseline OS distribution as a function of covariates. The probability density function that best describes the observed survival time was selected among normal, log-normal, Weibull, logistic, log-logistic, and exponential using the Akaike Information Criterion (22).

A "full" model was built by including all significant covariates from the Cox univariate analysis ($P < 0.05$, log-likelihood ratio test), and then a backward elimination was carried out. At each elimination step, the relative influence of each remaining covariate on the model was re-evaluated using a cutoff of $P < 0.01$ (12). If several of TGI metrics tested were significant in the Cox analysis, only the one with the best likelihood improvement was retained in the full model.

The POPLAR model was evaluated in simulating the POPLAR study (internal assessment) as well as BIRCH and OAK studies (external assessment)—conditional on patient baseline characteristics and tumor size data (estimated TGI metrics). OS distributions were simulated 1,000 times for patients with baseline

characteristics and KG estimates, as in the POPLAR, BIRCH, or OAK studies. OS model parameters were sampled from the estimated mean values and uncertainty in parameter estimates for each of the simulated study replicate. Censoring was simulated in sampling patient study duration in a uniform distribution based on observed censoring in the respective studies. For each replicate, Kaplan–Meier estimates of the simulated data as well as HR were calculated. The 95% prediction intervals across replicates were reported.

In addition, the outcome of OAK (OS HR) was simulated based on tumor kinetic data cutoff times from 10 to 122 weeks after the first patient was enrolled. For each of the data cutoffs, data from the patients recruited at this time (baseline characteristics, tumor size measurements, OS events) were collected and used to estimate (based on observed OS) or predict (with the model) HR. HR predictions were replicated 1,000 times to estimate the 95% prediction interval and the proportion of successful ($P < 0.05$) replicates. The simulation algorithm is described in Supplementary Fig. S1.

Results

Patients

To be evaluable, patients needed to have ≥ 1 postbaseline tumor size assessment. A total of 252 of the 277 patients randomized (91.0%) and 751 of the 850 patients randomized (88.4%) were evaluable in POPLAR and OAK, respectively. The patients were subjected to a median number of assessments of 4 (range, 2–13) over a median duration of 18 weeks (range, 3–82 weeks) in POPLAR and 4 (range 2–16) over a median duration 18 weeks (range, 1–108 weeks) in OAK.

TGI model

The longitudinal TGI model involved treatment arm–specific parameters for KS and KG. Any time lag (delay) on onset of effect implemented for all patients or as a mixture population model

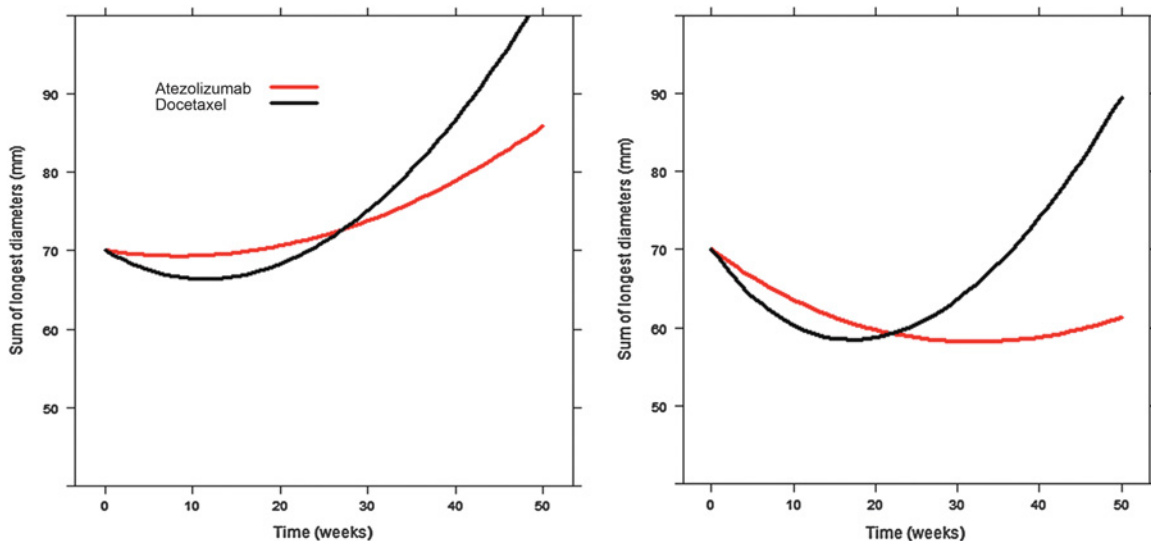


Figure 1.

Typical TGI profiles in the atezolizumab POPLAR study in all patients (left plot) and in the nonprogressors (right plot). Nonprogressors were defined as patients with model-predicted SLDs at week 6 \leq model-predicted SLDs at time 0 [start of treatment; $n = 83$ patients (67.5%) in the docetaxel arm and $n = 73$ patients (56.6%) in the atezolizumab arm].

was not identifiable (lag time estimate = 0 for 96.3% of patients with no improvement of the fit to the observed data). Final TGI model parameter estimates are shown in Supplementary Table S1, and the fit of individual tumor size data is illustrated in Supplementary Fig. S2. The model was flexible enough to accommodate the different patterns seen in the data.

All parameters are estimated precisely with a relative standard error < 20% for all parameters except for KS (< 30%). Bootstrap estimates of parameter of interest (i.e., those parameters that affect Bayesian estimates of individual parameters) were very similar, and this is true for point estimates of fixed-effect parameters and interpatient variances (from 0% to 3.2%) as well as shrinkage (from 0.3% to 8.0%). Those results denote the stability of the model estimation. Shrinkage was faster in the docetaxel arm (half-life [$\log(2)/KS$] of 31 weeks vs. 47 weeks, respectively), and growth was slower in the atezolizumab arm (tumor size doubling time [$\log(2)/KG$] of 48 weeks vs. 63 weeks, respectively, i.e., a 15-week or 3.4-month difference), as illustrated in Fig. 1 (left plot). In the nonprogressors, defined as patients with model-predicted SLD at week 6 \leq model-predicted SLD at time 0 [start of treatment; 83 patients (67.5%) in the docetaxel arm and 73 patients (56.6%) in the atezolizumab arm], deep and more durable shrinkage was observed in the atezolizumab arm with a 9.3-month longer doubling time (Fig. 1, right).

OS model

In a univariate Cox analysis of the POPLAR data (Table 1), $\log(KG)$ was the most significant (Supplementary Fig. S3) factor followed by TTG and ECTS and a number of baseline prognostic factors and treatment (atezolizumab vs. docetaxel). Among parametric models, the log-normal distribution had the best

Table 1. Cox univariate analysis of OS in 2L/3L patients with NSCLC in POPLAR

Covariate	Score ^a	P ^b	N ^c	Sign ^d
$\log(KG)$	69.4	<0.0001	252	+
TTG	46.7	<0.0001	252	-
ECTS week 8 ^e	37.6	<0.0001	252	+
Number of metastatic sites	28.2	<0.0001	252	+
ALP	20.2	<0.0001	247	+
Albumin	20.1	<0.0001	244	-
Baseline SLD	14.2	0.0002	252	+
Never smoker	6.8	0.0092	252	-
ECOG PS > 0	6.1	0.0139	252	+
Atezolizumab	5.7	0.0173	252	-
$\log(KS)$	5.1	0.0241	252	-
Nonsquamous disease	4.5	0.0346	252	-
Female	3.9	0.0495	252	-
Years since metastasis	3.7	0.0545	252	NA
TC123 or IC123	1.9	0.1688	252	NA
TC23 or IC23	1	0.3098	252	NA
AST	0.5	0.4787	247	NA
Age	0.4	0.546	252	NA
Total protein	0.4	0.5067	246	NA
LDH	0.3	0.6126	246	NA
Body weight	0.3	0.5997	249	NA

Abbreviations: ALP, alkaline phosphatase; ALT, alanine aminotransferase; AST, aspartate aminotransferase; ECOG PS, Eastern Cooperative Oncology performance status.

^aDifference in $-2 \times \log$ -likelihood between model with covariate and model with intercept only.

^bLog-likelihood ratio test.

^cNumber of patients with nonmissing covariate.

^dPositive sign in Cox model indicates that the hazard tends to increase with the covariate. NA: Not applicable when nonsignificant.

^eECTS weeks 12, 14, and 16 only marginally better.

Table 2. Parameter estimates of the final multivariate log-normal OS model in 2L/3L patients with NSCLC in POPLAR^a

Coefficients (unit)	Estimate ^b	SE	z	P value ^c
(Intercept)	1.22	0.600	2.04	0.0412
Number of metastatic sites	-0.163	0.0528	-3.09	0.00198
Albumin (g/L)	0.0519	0.0102	5.11	3.22e-07
$\log(KG)$ [week^{-1}]	-0.752	0.0875	-8.59	8.38e-18
$\log(\text{scale})^d$	-0.338	0.0639	-5.29	1.23e-07

Abbreviations: SE, standard error of parameter estimate; z, Wald statistic.

^aSurvival time was analyzed in days.

^bPositive value for the parameter estimate in log-normal model indicates that the hazard tends to decrease with the covariate.

^cDerived by using the Wald test (χ^2).

^dScale = SD of $\log(OS)$.

likelihood of describing the baseline OS distribution (Supplementary Table S2). After backward elimination, $\log(KG)$, number of metastatic sites and albumin level remained the only significant independent covariates in the final OS model (Table 2). According to this model, survival probability increases when the number of metastatic sites or KG decreases and albumin increases.

Evaluation of the model in simulating OS distributions in POPLAR is illustrated in Fig. 2. The TGI-OS POPLAR model was also evaluated by simulating OS HR in POPLAR and in OAK (conditional on patient's baseline characteristics and observed TGI profiles) in the general population and by PD-L1 expression (Fig. 3). Model assessment indicates good performance with observed HR within the 95% prediction intervals. Differences in $\log(KG)$ across arms captured the treatment effect (HR) in POPLAR and OAK in both the overall population and by PD-L1 expression when this PD-L1 expression was not in the final model. The TGI-OS POPLAR model was also able to predict OS distributions in PD-L1-positive patients in second-line plus patients and in first-line patients in BIRCH (Supplementary Fig. S4).

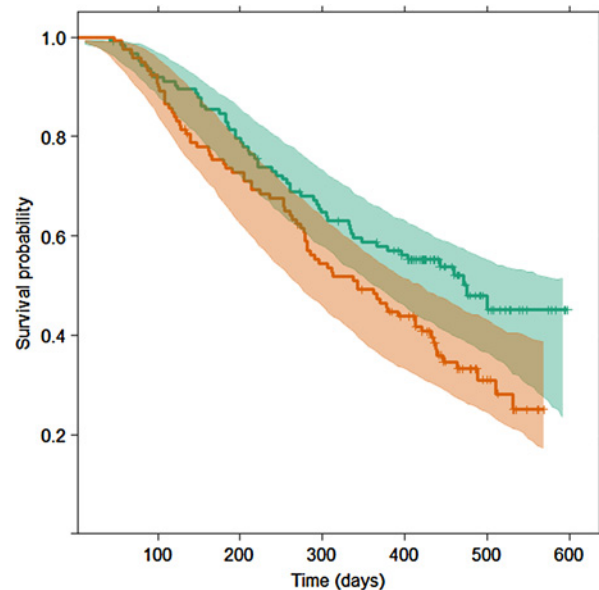


Figure 2.

TGI-OS POPLAR model prediction of OS distributions in POPLAR. Areas: 95% prediction interval of survival distributions; lines: observed Kaplan-Meier distributions with censored data (crosses) green: atezolizumab; orange: docetaxel.

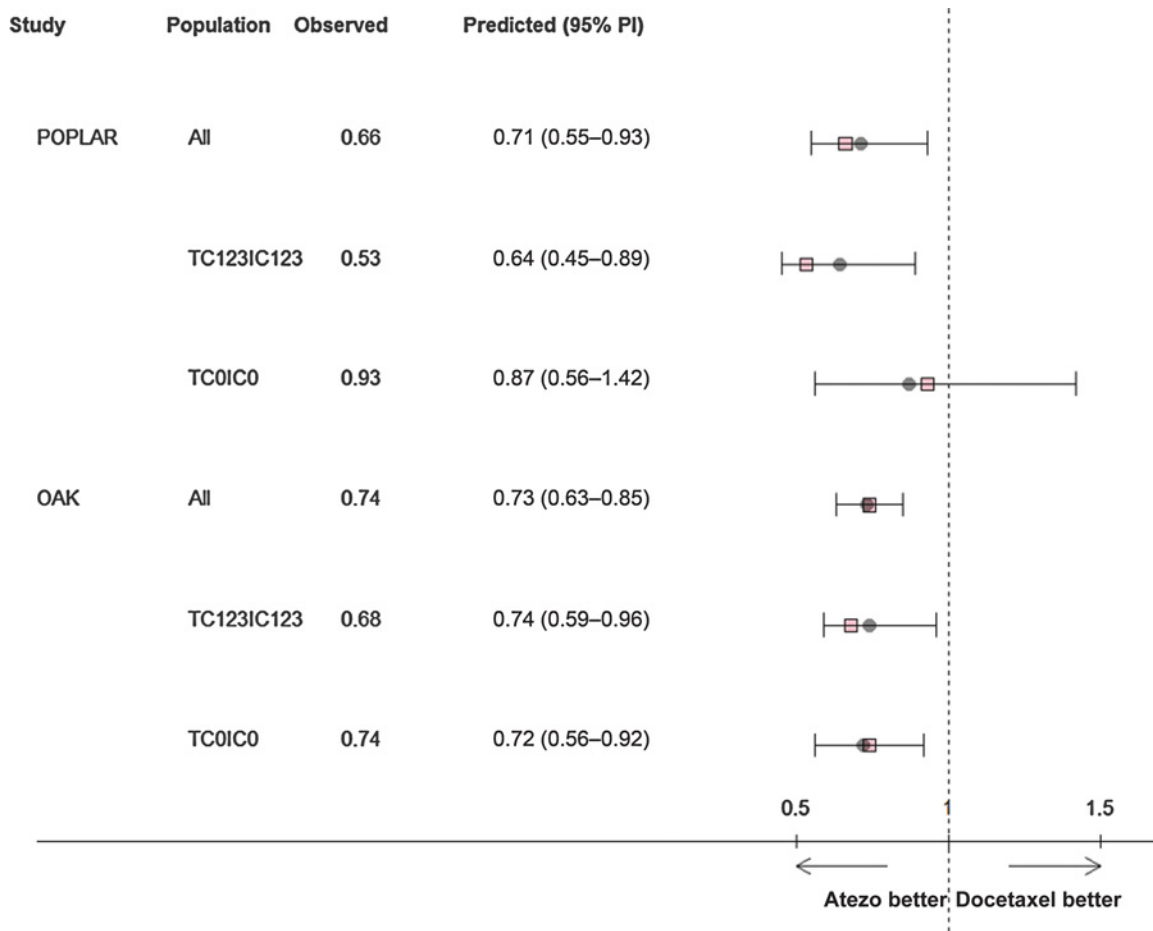


Figure 3.

TGI-OS POPLAR model prediction of the atezolizumab to docetaxel HR in the POPLAR and OAK studies in all patients and by biomarker expression (PD-L1; simulation of 1,000 replicates vs. observed). Model-predicted HRs (circles) and 95% prediction intervals (PIs; bars) with observed HRs (squares). TC123IC123: patients with PD-L1 expression 1, 2, or 3 in either TCs or ICs; TC0IC0: patients with PD-L1 expression 0 in TC and IC.

OAK outcome prediction based on early TGI data

Model-predicted and observed OS HR in OAK, based on data cutoffs as a function of study time varying from 10 to 120 weeks since the first patient was enrolled, are shown in Supplementary Fig. S5 and summarized in Table 3 (25 to 80 weeks only).

The results in Supplementary Fig. S5 indicate unreliable predictions as well as unstable observed OS for early data

cutoffs (<40 weeks). As data accrue, model-predicted as well as observed HR stabilized around the final study estimate (at times > 80 weeks). The model predicted the final HR from 40 weeks onward after the first patient was enrolled with >97% successful (significant) studies across the 1,000 replicates when a successful study was predicted from 70 weeks onward based on observed OS (Table 3). At 40 weeks, all patients entered the study, but only half of the tumor size data were available due to the shorter follow-up.

Table 3. Model-predicted 95% CI (% of significant replicates) across 1,000 replicated studies and observed OS HR in the OAK study based on data cutoffs at times varying from 25 to 80 weeks since the first patient was treated

Data cut (weeks)	Model-based predictions		Observed	
	HR (95% CI)	Success (%)	HR (95% CI)	P
25	0.99 (0.85–1.15)	4.8	0.91 (0.43–1.96)	0.818
30	0.81 (0.69–0.94)	78.5	0.91 (0.53–1.55)	0.717
40	0.67 (0.56–0.80)	99.3 ^a	0.84 (0.59–1.21)	0.347
50	0.66 (0.56–0.78)	99.8	0.82 (0.63–1.08)	0.152
60	0.68 (0.58–0.80)	100.0	0.80 (0.64–1.00)	0.053
70	0.72 (0.61–0.85)	97.1	0.77 (0.62–0.95)	0.012 ^b
80	0.71 (0.60–0.84)	98.4	0.74 (0.60–0.89)	0.002

NOTE: Success: % of replicates with $P < 0.05$; P value measured by Cox analysis.

^aPredicts >97% success from 40 weeks onward.

^bPredicts success from 70 weeks onward.

Discussion

Although previous TGI-OS models were successful in capturing the direct action of chemotherapeutics and targeted agents on tumors (11–15), it remained unclear whether we could apply these models for CIT (which acts on the immune system) when discordance is observed between ORR/PFS and OS. In this study, we modeled TGI profiles (sum of target lesions per RECIST 1.1) observed in both arms of the POPLAR study. We did not find strong evidence of delayed responses or pseudoprogessions at the population level based on target lesions consistent with the phase I KEYNOTE-001 study with pembrolizumab (23). TGI profiles in

Downloaded from http://aacrjournals.org/clinccancerres/article-pdf/24/14/3292/2044574/3292.pdf by guest on 08 November 2024

the atezolizumab and docetaxel arm, as illustrated in Fig. 1, crossed at about 25 weeks, with more initial shrinkage with docetaxel and slower KG with atezolizumab and the difference in KG, whether related to durable response or prolonged stable disease, accounted for the difference in OS (HR) observed in the two treatment groups. The model therefore predicts benefit with atezolizumab treatment in both responders and nonresponders. The model was able to predict the increasing improvement in OS HR associated with increasing baseline PD-L1 expression in tumors or in tumor-infiltrating ICs observed in POPLAR (7), even though this biomarker was not included in the TGI-OS model. This suggests that differences in growth rate constant across patients captured the atezolizumab treatment effect across sub-populations with varying biomarker expressions. The POPLAR TGI-OS model was also able to predict outcome in external studies (not used to develop the model), including OAK in a similar all-comer second- and third-line population and in BIRCH in PD-L1-positive first-line, second-line, and third-line patients treated with atezolizumab, suggesting that the KG-OS link is robust across populations and lines of therapies. Furthermore, the POPLAR TGI-OS model was able to predict OAK outcome (HR) based on baseline characteristic and longitudinal tumor size data at 40 weeks after the first patient was enrolled, at which time only half of the tumor size assessments were available. This result is conditional on OAK study design, accrual rate, censoring, and outcome.

Other TGI metrics (TTG, ECTS, and KS), although correlated with OS (as shown in other NSCLC studies; refs. 11–15), did not predict the observed difference in OS in those particular studies comparing an immunotherapy with chemotherapy consistent with the typical tumor profiles that are crossing during treatment. In a previous work (12), log(KG) was found to predict bevacizumab treatment effect in patients with colorectal cancer as well as TTG.

This novel approach combined with immune biomarker profiling may help shed light into the complex interplay between an individual's "cancer-immune set point" and CIT response (24) by providing a sensitive exploratory endpoint (compared with probability of response and PFS) to help assess predictive baseline biomarkers, one of the major challenges in oncology in general and for immunotherapies in particular. Champiat and colleagues (25) recently reported that patients with a variety of tumor types treated in phase I studies may show very fast progression on anti-PD-1/PD-L1 by comparing pretreatment with on-treatment growth rate constants. We could not address this question with our data set for patients who had only one pretreatment (baseline) scan as typical in clinical trial data, precluding any estimate of pretreatment growth.

In conclusion, this was the first study to show that the on-treatment TGI metric growth rate constant can predict outcomes (OS HR) for CIT molecules. Furthermore, the TGI-OS model appears to be robust enough to predict outcomes in patients who received varying extent of prior therapies and with various PD-L1 expressions at baseline. The growth rate constant

may be a promising "on-treatment model-based biomarker" of OS for CIT and have utility as an early radiographic efficacy measure when ORR and PFS show no significant difference across treatments, such as in both the POPLAR and OAK studies (7, 8). Accordingly, the proposed modeling framework may also have value in supporting the design and analysis of early clinical as well as of pivotal studies with CIT and help prioritize and select the most promising combination therapies (with slowest growth) and optimal doses for these agents. Decisions might be based on an estimate of change in KG (decrease in growth rate) for an investigational treatment compared with control (26). The operating characteristics of KG as an endpoint are being investigated.

Disclosure of Potential Conflicts of Interest

L. Claret and R. Bruno were employees of Pharsight Consulting Services and paid contractors for Genentech/Roche when part of this research was conducted. L. Claret, J.Y. Jin, H. Winter, S. Girish, M. Stroh, P. He, M. Ballinger, A. Joshi, and R. Bruno are full-time employees of Genentech/Roche and may hold stocks or stock options. A. Rittmeyer received grants as an advisor or speaker for AstraZeneca, Bristol-Myers Squibb, Boehringer Ingelheim, Eli Lilly, Pfizer, and Genentech/Roche. D. Gandara consulted for and received clinical trial grants from Genentech. J.-C. Soria received consultancy fees from AstraZeneca, Astex, Clovis, GSK, Gammababs, Lilly, MSD, Mission Therapeutics, Merus, Pfizer, PharmaMar, Pierre Fabre, Roche-Genentech, Sanofi, Servier, Symphogen, and Takeda. No potential conflicts of interest were disclosed by the other authors.

Authors' Contributions

Conception and design: L. Claret, J.Y. Jin, C. Ferté, S. Girish, P. He, D. Gandara, J.-C. Soria, R. Bruno

Development of methodology: L. Claret, J.Y. Jin, C. Ferté, D. Gandara, R. Bruno

Acquisition of data (provided animals, acquired and managed patients, provided facilities, etc.): M. Ballinger, A. Rittmeyer, D. Gandara, R. Bruno

Analysis and interpretation of data (e.g., statistical analysis, biostatistics, computational analysis): L. Claret, C. Ferté, H. Winter, S. Girish, M. Stroh, P. He, M. Ballinger, A. Rittmeyer, D. Gandara, J.-C. Soria, R. Bruno

Writing, review, and/or revision of the manuscript: L. Claret, J.Y. Jin, C. Ferté, H. Winter, S. Girish, M. Stroh, P. He, M. Ballinger, A. Sandler, A. Joshi, A. Rittmeyer, D. Gandara, J.-C. Soria, R. Bruno

Administrative, technical, or material support (i.e., reporting or organizing data, constructing databases): L. Claret, C. Ferté, A. Rittmeyer, D. Gandara, R. Bruno

Study supervision: L. Claret, P. He, M. Ballinger, A. Sandler, D. Gandara, R. Bruno

Acknowledgments

This work was supported by Genentech, Research and Early Development.

The authors thank all the patients who participated in these studies, the participating research nurses and data coordinators, Mathilde Marchand Certara, Strategic Consulting, Wan-Ting Lin, Sheila Dayog, Roche/Genentech Clinical Pharmacology, and the Atezolizumab Project Team.

The costs of publication of this article were defrayed in part by the payment of page charges. This article must therefore be hereby marked *advertisement* in accordance with 18 U.S.C. Section 1734 solely to indicate this fact.

Received December 8, 2017; revised February 22, 2018; accepted April 17, 2018; published first April 23, 2018.

References

- Chen DS, Irving BA, Hodi FS. Molecular pathways: next-generation immunotherapy-inhibiting programmed death-ligand 1 and programmed death-1. *Clin Cancer Res* 2012;18:6580–7.
- Zou W, Chen L. Inhibitory B7-family molecules in the tumour microenvironment. *Nat Rev Immunol* 2008;8:467–77.
- Chen DS, Mellman I. Oncology meets immunology: the cancer-immunity cycle. *Immunity* 2013;39:1–10.
- Herbst RS, Soria JC, Kowanetz M, Fine GD, Hamid O, Gordon MS, et al. Predictive correlates of response to the anti-PD-L1 antibody MPDL3280A in cancer patients. *Nature* 2014;515:563–7.

5. Matsumoto K, Fukuyama S, Eguchi-Tsuda M, Nakano T, Matsumoto T, Matsumura M, et al. B7-DC induced by IL-13 works as a feedback regulator in the effector phase of allergic asthma. *Biochem Biophys Res Commun* 2008;365:170–5.
6. Akbari O, Stock P, Singh AK, Lombardi V, Lee WL, Freeman GJ, et al. PD-L1 and PD-L2 modulate airway inflammation and iNKT-cell-dependent airway hyperreactivity in opposing directions. *Mucosal Immunol* 2010;3:81–91.
7. Fehrenbacher L, Spira A, Ballinger M, Kowanetz M, Vansteenkiste J, Mazieres J, et al. Atezolizumab versus docetaxel for patients with previously treated non-small-cell lung cancer (POPLAR): a multicentre, open-label, phase 2 randomised controlled trial. *Lancet* 2016;387:1837–46.
8. Rittmeyer A, Barlesi F, Waterkamp D, Park K, Ciardiello F, von Pawel, et al. Atezolizumab versus docetaxel in patients with previously treated non-small-cell lung cancer (OAK): a phase 3, open-label, multicentre randomised controlled trial. *Lancet* 2017;389:255–65.
9. Peters S, Gettinger S, Johnson ML, Jänne PA, Garassino MC, Christoph D, et al. Phase II trial of atezolizumab as first-line or subsequent therapy for patients with programmed death-ligand 1-selected advanced non-small-cell lung cancer (BIRCH). *J Clin Oncol* 2017;35:2781–9.
10. Therasse P, Arbuck SG, Eisenhauer EA, Wanders J, Kaplan RS, Rubinstein L, et al. New guidelines to evaluate the response to treatment in solid tumors. European Organization for Research and Treatment of Cancer, National Cancer Institute of the United States, National Cancer Institute of Canada. *J Natl Cancer Inst* 2000;92:205–16.
11. Claret L, Girard P, Hoff PM, Van Cutsem E, Zuideveld KP, Jorga K, et al. Model-based prediction of phase III overall survival in colorectal cancer on the basis of phase II tumor dynamics. *J Clin Oncol* 2009;27:4103–8.
12. Claret L, Gupta M, Han K, Joshi A, Sarapa N, He J, et al. Evaluation of tumor-size response metrics to predict overall survival in Western and Chinese patients with first-line metastatic colorectal cancer. *J Clin Oncol* 2013; 31:2110–4.
13. Wang Y, Sung C, Dartois C, Ramchandani R, Booth BP, Rock E, et al. Elucidation of relationship between tumor size and survival in non-small-cell lung cancer patients can aid early decision making in clinical drug development. *Clin Pharmacol Ther* 2009;86:167–74.
14. Claret L, Bruno R, Lu JF, Sun YN, Hsu CP. Exploratory modeling and simulation to support development of motesanib in Asian patients with non-small cell lung cancer based on MONET1 study results. *Clin Pharmacol Ther* 2014;95:446–51.
15. Bruno R, Mercier F, Claret L. Evaluation of tumor size response metrics to predict survival in oncology clinical trials. *Clin Pharmacol Ther* 2014;95: 386–93.
16. Wolchok JD, Hoos A, O'Day S, Weber JS, Hamid O, Lebbé C, et al. Guidelines for the evaluation of immune therapy activity in solid tumors: immune-related response criteria. *Clin Cancer Res* 2009;15:7412–20.
17. Chiou VL, Burotto M. Pseudoprogression and immune-related response in solid tumors. *J Clin Oncol* 2015;33:3541–3.
18. Hodi FS, Hwu WJ, Kefford R, Weber JS, Daud A, Hamid O, et al. Evaluation of immune-related response criteria and RECIST v1.1 in patients with advanced melanoma treated with pembrolizumab. *J Clin Oncol* 2016;34: 1510–7.
19. Seymour L, Bogaerts J, Perrone A, Ford R, Schwartz LH, Mandrekas S, et al. iRECIST: guidelines for response criteria for use in trials testing immunotherapeutics. *Lancet Oncol* 2017;18:e143–e152.
20. Stein WD, Gulley JL, Schlom J, Madan RA, Dahut W, Figg WD, et al. Tumor regression and growth rates determined in five intramural NCI prostate cancer trials: the growth rate constant as an indicator of therapeutic efficacy. *Clin Cancer Res* 2011;17:907–17.
21. Beal SL, Sheiner LB. NONMEM User's Guides. NONMEM Project Group. San Francisco, CA: University of California at San Francisco; 1992.
22. Akaike H. A new look at the statistical model identification. *IEEE Trans Automat Contr* 1974;19:716–23.
23. Chatterjee M, Turner DC, Felip E, Lena H, Cappuzzo F, Horn L, et al. Systematic evaluation of pembrolizumab dosing in patients with advanced non-small-cell lung cancer. *Ann Oncol* 2016;27:1291–8.
24. Chen DS, Mellman I. Elements of cancer immunity and the cancer-immune set point. *Nature* 2017;541:321–30.
25. Champiat S, Derle L, Ammari S, Massard C, Hollebecque A, Postel-Vinay S, et al. Hyperprogressive disease is a new pattern of progression in cancer patients treated by anti-PD-1/PD-L1. *Clin Cancer Res* 2017;23:1920–8.
26. Bruno R, Claret L, Jin YJ, Girish S. Applications of tumor growth inhibition-overall survival models to support atezolizumab combination studies [cited 2018 May 24]. Available from: <https://www.fda.gov/Drugs/NewsEvents/ucm589449.htm>.